Journal of Water Process Engineering 47 (2022) 102786

Contents lists available at ScienceDirect

Journal of Water Process Engineering

journal homepage: www.elsevier.com/locate/jwpe

Innovative capacitive deionization-degaussing approach for improving adsorption/desorption for macadamia nutshell biochar

Raed A. Al-Juboori [a,*], Salam Bakly [b], Les Bowtell [c], Susan S.A. Alkurdi [d], Ali Altaee [b]

[a] Water and Environmental Engineering Research Group, Department of Built Environment, Aalto University, P.O. Box 15200, Aalto, FI-00076 Espoo, Finland
[b] Centre for Green Technology, School of Civil and Environmental Engineering, University of Technology Sydney, 15 Broadway, Sydney, NSW 2007, Australia
[c] Faculty of Health, Engineering and Sciences, University of Southern Queensland, Toowoomba, QLD 4350, Australia
[d] Northern Technical University, Engineering Technical College, Kirkuk, Iraq

ARTICLE INFO

Keywords:
Macadamia nutshell biochar (MBC)
Nitrate
Fixed-bed adsorption
CDI and degaussing

ABSTRACT

Adsorption is a well known effective technology for water treatment. Although limited capacities of adsorbents and regeneration issues are two common challenges. This study proposed and tested innovative approaches for improving adsorption/desorption of biochar made from macadamia nutshell (MBC). These approaches are capacitive deionization (CDI) and degaussing (full process detailed in methods), for the respective enhancement of adsorption and desorption of MBC. Nitrate was used as a model contaminant. It was found that CDI could extend the saturation time of MBC by increasing the bed specific throughput by 10 fold. Modeling of the breakthrough curves showed that the modified dose-response model fits well the experimental data. The regeneration of MBC with degaussing and deionized water backwash was compared with conventional tap and deionized water backwash. Degaussing increased the maximum nitrate recovery for deionized water from 50% to 73%. In comparison, the maximum nitrate recovery with tap water was 23%. The degaussing improvement of nitrate desorption holds for only the first 60 min. The obtained charge efficiency for MBC-CDI was slightly higher than literature values for the same applied voltage (78,6%). The degaussing system was also proven to be efficient with energy consumption of 43,7 J/mmol of NO_3^-. The possible mechanism behind degaussing improvement of nitrate desorption is the removal of the static charges on nitrate ion hydration. The regenerated MBC with degaussing and deionized water was tested with CDI for nitrate adsorption and compared to fresh MBC. The regenerated MBC-CDI exhibited better nitrate adsorption than fresh MBC for two cycles.

1. Introduction

Chemical fertilizer application and wastewater discharge are among the main factors contributing to the increase of nitrogen loaded in watershed [1]. Urban runoff carries nutrients from unutilized fertilizers in agricultural fields, sanitary plants or animal wastes to water resources. The mitigation of N oxides (NO_3^-) to groundwater and surface runoff has deteriorated water quality and may lead to hypoxia conditions [2]. The accumulation of nitrogen oxides from the atmosphere to sea and land can damage water bodies through eutrophication [3]. The excess NO_3^- in drinking water threatens human health and has been linked to several diseases such as diabetes, methemoglobinemia, stomach cancer and thyroid disorders [2,4].

Numerous physical and chemical techniques have been used for nitrate removal from aqueous solutions. These include filtration, coagulation, chemical reduction, electrodialysis, biological techniques, ion exchange and adsorption [5,6]. Most of these methods either require high cost, long processing time or produce high volume of sludge. Unlike these methods, adsorption is relatively fast and requires minimal energy. Adsorption can be applied using low-cost waste material such as biochar, which can easily be regenerated [7]. The renderability of adsorbents allows reducing the volume of the sludge produced from the process, and also offers opportunities of recovering adsorbate.

In recent years, biochar has gained great attention due to its environmental applications in the field of water and wastewater treatment. It was used to remove a wide range of organic, inorganic and heavy metals/metalloids [8–10]. Biochar is a carbon-rich material produced from biomass's thermochemical conversion in the absence of or in an oxygen-limited environment [11]. The temperature ranges for the thermochemical conversion of biomass are 300–700 °C and

* Corresponding author.
E-mail address: raed.al-juboori@aalto.fi (R.A. Al-Juboori).

https://doi.org/10.1016/j.jwpe.2022.102786
Received 26 September 2021; Received in revised form 7 February 2022; Accepted 9 April 2022
Available online 29 April 2022

500–1000 °C in the case of slow and fast pyrolysis, respectively, 750–900 °C for gasification, 180–300 °C for hydrothermal carbonization, 290 °C for torrefaction and 300–600 °C for flash carbonization [12]. The yield of biochar and its chemical and physical properties are directly related to the process adopted for its production (temperature, residence time and heating rate) and the biomass used. The latter may range from agricultural and forestry residues, wood waste, animal manure, sludge waste, etc. [12].

Currently, much attention has been paid to the recirculation of macadamia waste into adsorbents for water/wastewater treatment [13,14]. Macadamia nutshell is a lignocellulose waste material resulting from the macadamia nut processing. The amount produced worldwide is about 44,000 metric tonnes in kernel form, with 86% of the total amount produced in Australia [15]. The amount recycled as fuel or garden mulch was reported to be 5000 tonnes of the overall produced waste, while the rest was discarded as a solid waste [16]. The thermal conversion of macadamia nutshell into biochar was addressed as a vital waste recycling method [17]. Macadamia nutshell biochar (MBC) is a highly porous material with large surface area and active surface functional groups, such as carbonyl and hydroxyl [17]. The high surface area of MBC makes it an effective adsorbent for nitrate. Yang et al. found that nitrate adsorption into biochar produced from different agricultural waste is directly related to the surface area [6]. Macadamia nutshell was rarely examined for the removal of nitrate from water. Limited studies examined the MBC's nitrate removal capacity, mostly conducted in bioreactor systems [18,19]. Our research team conducted one of the very few studies that examined nitrate removal with MBC in a column system [20]. Two research questions arose from this work: the possibility of improving the adsorption capacity of MBC and its regeneration using chemical-free techniques. Most of the regeneration and adsorption improvement methods rely either on using chemicals such as NaOH, H_2O_2, solvents etc. or high energy techniques (thermal regeneration). Using chemical regeneration methods contributes to the discharge of more pollutants into the environment. In some cases, highly toxic and costly chemicals may be needed for the regeneration process [21]. Therefore, it is crucial to investigate innovative, environmentally friendly methods for enhancing the adsorption and regeneration of biochar.

This study proposes a novel cost-effective approach of applying Capacitive De-Ionization (CDI) and a unique degaussing technique for improving the adsorption and desorption capacity of MBC using nitrate as a model contaminate. CDI is an environmentally safe and cost-effective method that was originally used for the desalination of saline water. The principle of the process is based on the electric double layer theory, in which two different charges will be provided to two porous carbon electrodes, thus attracting the dissolved ions in the solution [22]. The common techniques for regenerating CDI are short circuit, reduced potential and polarity reversal [23]. Although these techniques do not generate secondary waste, they still have some shortcomings, or they do not suit the proposed system setup in this study. For instance, short-circuit and reduced potential have low regeneration efficiency and long desorption times [24,25]. Polarity reversal is not suitable for the case of this study as the system does not include a selective membrane to prevent ions being transported to oppositely charged electrodes. Therefore, degaussing has been proposed in this study to test as a new regeneration technique. Degaussing is an existing technique that has mostly been used to remove static magnetic fields from ships or in more recent times from cathode ray tube (CRT) displays. The concept of this technique is that any residual static magnetic field is removed when a stronger alternating magnetic field (of no DC or average bias) is applied. In this study following a similar approach to static charge rather than magnetic field, a stronger AC voltage is applied to remove any residual charges in the carbon elements. Looking at the CDI system as an equivalent electrical circuit it may be seen as a capacitor with a number of parallel plates. In order to remove any residual or DC component, a degaussing AC signal of approximately an order of magnitude higher is applied. The purpose of CDI in this study is to improve nitrate adsorption onto the MBC column by boosting electrostatic interactions. The column behaviour with and without CDI was studied using common breakthrough curve models. The effect of CDI incorporation on column performance indicators such as carbon usage rate and specific throughput was also assessed. The degaussing was coupled with a deionized water backflush to collect the desorbed nitrate from MBC. The regeneration with degaussing will be benchmarked with tap and deionized water regeneration alone. The capacity of the regenerated column for nitrate adsorption was evaluated for two cycles in this study.

2. Materials and methods

2.1. Solution preparation

As highlighted in the introduction that nitrate has been selected as a model contaminant in this study. A 100 mg/L of nitrate stock solution was prepared by dissolving 135.4 mg of sodium nitrate analytical reagent grade (Chem-Supply, Australia) in 1 L of distilled water. This stock solution was prepared to save time, reduce storage space, conserve materials and improve the accuracy of dilution series preparation. It was found in our previous study on nitrate removal with MBC that the highest applied concentration of 15 mg/L resulted in the highest removal [20], and this concentration level was applied in this investigation.

2.2. Biochar preparation

MBC was used in this study for investigating nitrate removal and bed regeneration. Details of MBC preparation and characterization are provided in our previous work [20]; it is important to highlight the char's preparation conditions and characteristics briefly. MBC was prepared in-house under slow pyrolysis at 1000 °C using a kiln (Rio Grande PMC Model #703-118, Rio Grande, Albuquerque, NM, USA). MBC prepared at 1000 °C is characterized by its porous structure, high crystallinity, high carbon content of more than 90% and presence of hydroxyl and carboxylic groups.

2.3. Preparation of carbon electrode

Carbon is widely used for preparing CDI electrodes due to its low contact resistance, low cost, high electrical conductivity and practicality. In this study, carbon electrodes were extracted from 6 V Eveready heavy duty batteries. The electrodes were cleaned, then sterilized with ethanol and covered with copper caps. The electrodes were connected to two linear power supplies, GwInstek model GPC-3030D for the CDI mode of operation.

2.4. MBC-CDI column setup

A plastic column with an internal diameter of 3.85 cm and a height of 14 cm was used to conduct the experimental work. The column was packed with MBC to a bed height of 12.20 cm. Six holes were made on two sides of the column for embedding the electrodes into the biochar, as presented in Fig. 1. The three right holes were made at distances of 1, 5 and 9 cm from the bottom of the column, while the three left holes distance from the bottom were 3, 7 and 11 cm, respectively. The column was packed with 46.3 g of MBC in stages, where each electrode was inserted into the column at the set depth and covered with biochar. A fibreglass screen was laid on top of each layer to separate them and prevent MBC particles transport across the layers. Each electrode was glued to the column with commercial silicon to prevent leakage. The same process was repeated for the rest of the biochar layers and electrodes. Once the column was packed with MBC and the six-carbon electrodes, the top of the column was covered with doubled fibreglass screen to prevent MBC particles escaping to the filtrate tank. The column

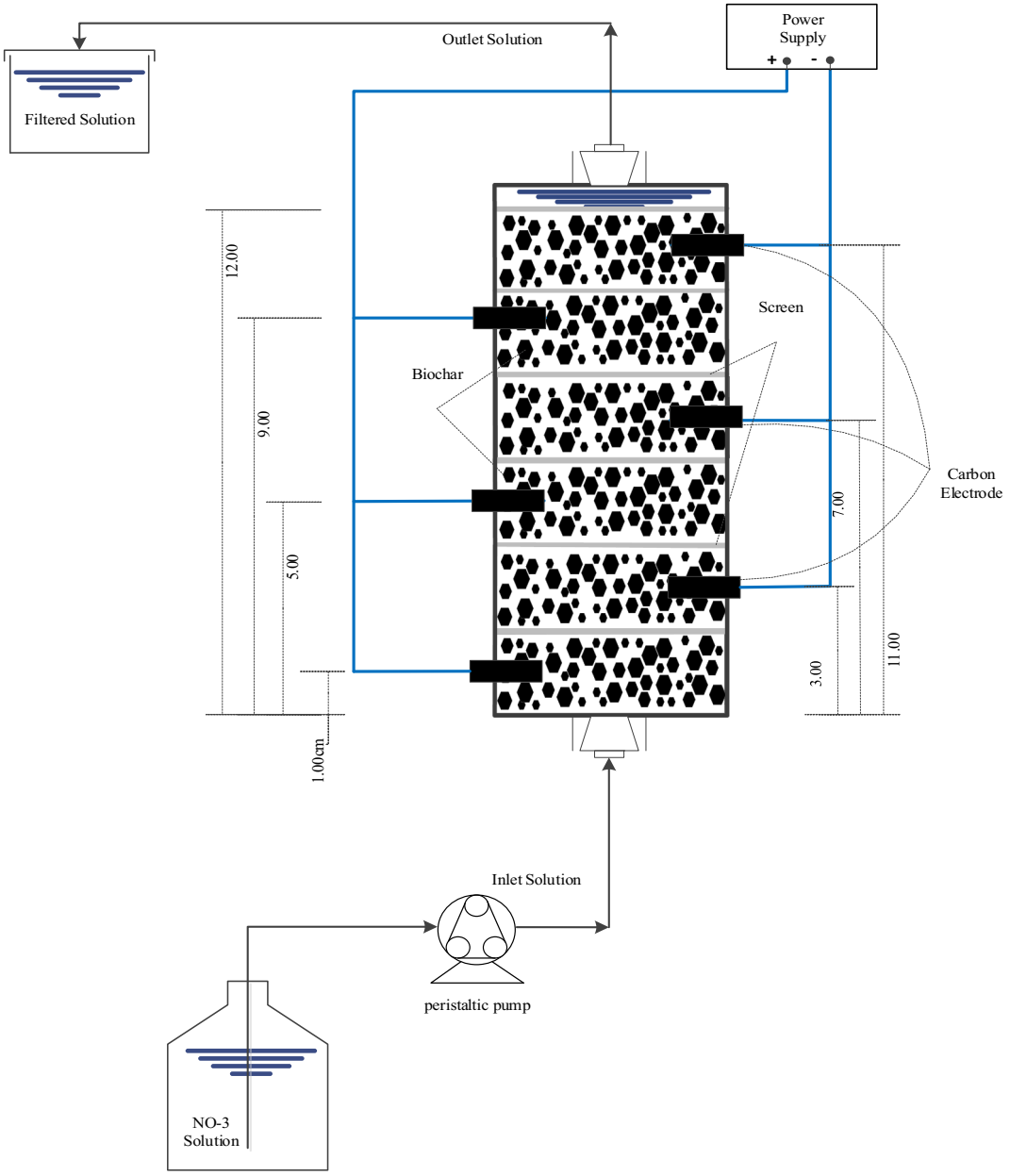

Fig. 1. MBC-CDI filtration column.

was sealed from the top and the bottom using plastic caps and silicon. The feed and discharge tanks were connected to the column using silicon tubes. Twenty-litre, sterilized plastic containers were used to carry the feed solution and the filtrate. The feed solution was pumped into the bottom of the column using a Masterflex peristaltic pump (model no. 7520-47, USA). The electrodes were connected to the power supply (Farnell, Stabilized power supply L30-2) to provide the system with a voltage of 1.2 V, with current decreasing over time. The applied CDI parameters were chosen at these levels to avoid the occurrence of some technical problems such as the increase of pH, scale deposition on electrodes, water electrolysis near the electrode and high energy consumption. The equivalent capacitance of the system was determined using a Fluke 289 multimeter system, yielding approximately 500 μF. It is worth mentioning that the possibility of inter-cell short circuiting was tested by measuring the current drawn by a dry column to check if any direct contact was made across the fibreglass screen. In addition, the same test was done with deionized water flowing through the CDI cell and checked that current drawn was negligible i.e. <0.00 mA. The same setup explained above was used for performing the regeneration experiments, except that the feed solution was replaced with backflush water (tap water or deionized water, denoted as TW and DW, respectively).

2.5. MBC-CDI nitrate removal procedure

Nitrate solution was fed to the MBC-CDI column at a flowrate of 2 mL/min. At the same time, the power supplies were turned on to start the electro-sorption process. The solution was single passed upward through the column for 72 h and samples were taken at 5, 15, 30, 60, 120, 180, 240, 300, 360, 720, 1440, 2880 and 4320 min to find the best removal timeframe as this would help in defining the effective operating conditions and accurately finding the saturation point of the column. The adsorption tests with MBC alone were performed using the same setup. This means that MBC tests accounted for physical adsorption by both biochar and electrode materials.

2.6. Regeneration scenarios

As discussed in the introduction section, a decent part of this study is intended to test the performance of proposed chemical-free electrical regeneration techniques compared to traditional backflush techniques. This study proposed using degaussing as an external shock to induce the desorption of nitrate from the MBC-CDI bed. The degaussing conditions applied in this work are 100 Hz frequency square waveform with amplitude of 7.5 V with power drawn decreasing over time from 45 mW to 15 mW. The regeneration experiments were conducted on the saturated MBC-CDI column. The same flow conditions and sample collection routine as those applied in the removal experiments were repeated in the regeneration treatments. It is noteworthy that two types for flushing water were tested: DW for simulating lab environments and TW for simulating practical, real-life applications. It is important to emphasis that the purpose of using TW and DW in this study was to serve as a benchmark for evaluating degaussing technique rather than testing them as regeneration techniques for biochar columns. TW might be used alone or for diluting regeneration chemicals in reallife small-scale applications, but DW is an unlikely option for such a use due to its high cost. The regeneration with only TW and DW was performed for 2 cycles, while with degaussing for 3 cycles. The goal of the regeneration tests was to examine preliminarily performance of the proposed degaussing technique versus the conventional flush with water approach. Although a limited number of cycles were applied in this study, this was deemed acceptable, especially in that our study is testing this technique for the first time and the focus was on studying the possibility of applying it in biochar columns. There are many examples of studies in the literature where a limited number of regeneration cycles (up to 3) were applied particularly when new applications or adsorbents were under investigation such as the studies reported in [26,27]. The regenerated columns with degaussing were tested again for nitrate removal for at least two cycles. All experiments were conducted in triplicate in this study, and results will be presented in mean values with standard error values stated.

2.7. Nitrate measurements

The removal capacity denoted as q_t (mg/g MBC) of nitrate was determined by applying Eq. (1). Ion chromatography ICS-2000 system (Dionex-Thermo Fisher, Melbourne, Australia) was utilized for measuring nitrate concentration in the collected samples applying standard method 4110B detailed in [28].

$$q_t = \frac{(C_0 - C_t)^* V}{X} \quad (1)$$

2.8. Fixed-bed sorption models

The column performance and adsorption behaviour are commonly studied using the relationship between adsorbate concentration and time, called the breakthrough curve (BTC) [29]. An adequate prediction of BTC for given operating conditions plays an important role in designing fixed-bed column adsorption systems [30]. This can be done by utilizing practical, simplified models developed to study adsorbate-adsorbent's dynamic behaviour in fixed-bed columns systems. This study examined nitrate adsorption behaviour onto MBC and MBC-CDI columns using six commonly used fixed-bed adsorption models in their none-liner and liner formats. The mathematical formulae of these models are presented in Table 1. The definition of the parameters of these models and other formulae applied in this work is provided in the nomenclature section.

A brief discussion of the applied fixed bed models are provided here. The Bohart-Adam model carries the names of the two scientists who developed it for studying the removal of chlorine from the air using a charcoal column. The model is based on the assumption that adsorption rate is directly related to the concentration of adsorbate and the residual capacity of adsorbent [31]. Thomas derived a model for studying the adsorption process in a fixed-bed column using the Langmuir isotherm and second-order reaction kinetics [32,33]. The Yoon-Nelson model was developed to investigate gaseous adsorption onto respirator cartridges [34]. The main premise of this model is that the rate of decrease in the probability of adsorbate adsorption is proportional to the probability of the adsorbate adsorption and breakthrough on the adsorbent [29]. This model is relatively simple compared to other fixed-bed models, as it does not require knowledge of the adsorbate and adsorbent characteristics [35]. The development of the Clark model was based on the Freundlich isotherm and mass transfer concept [36]. The purpose of developing this model was to evaluate the performance of granular activated carbon filters for removing pollutants in drinking water treatment systems. The adsorption of pollutants onto activated carbon motivated Wolborska to develop a fixed-bed model based on mass transfer concepts for low concentration breakthrough curves [37]. The model is simplified to its popular format shown in Table 1 with the assumption of negligible axial diffusion, which is likely the case for short columns and high solution flow rates. Yan and co-workers developed the modified dose-response model to find a fit better than Bohart-Adam and Thomas models for metal adsorption onto fixed-bed of biomaterials [38]. The model is empirical, and it is based on the formula of logistics model in statistics that is analogous to typical breakthrough curve in fixed-bed systems.

The goodness of fit for the models experimental data was evaluated by determining the coefficient of determination (R^2), Chi-square coefficient (χ^2) and the sum of square error (SSE).

Table 1
Applied fixed-bed models in this study.

Models	None-linear form	Linear form	Equation no.	Reference
Bohart-Adam	$\frac{C_t}{C_0} = \frac{e^{k_{BA}C_0 t}}{e^{k_{BA}N_0\frac{Z}{U}} - 1 + e^{k_{BA}C_0 t}}$	$ln\left(\frac{C_0}{C_t} - 1\right) = ln\left[e^{k_{BA}N_0\frac{Z}{U}} - 1\right] - k_{BA}C_0 t$	(2)	[31]
Thomas	$\frac{C_t}{C_0} = \frac{1}{e^{\frac{k_T q_0 X}{Q} - k_T C_0 t} + 1}$	$ln\left(\frac{C_0}{C_t} - 1\right) = \frac{k_T q_0 X}{Q} - k_T C_0 t$	(3)	[33]
Yoon-Nelson	$\frac{C_t}{C_0} = \frac{1}{e^{k_{YN}(\tau - t)} + 1}$	$ln\left(\frac{C_0}{C_t} - 1\right) = k_{YN}\tau - k_{YN}t$	(4)	[34]
Clark	$\frac{C_t}{C_0} = \left(\frac{1}{Ae^{-rt} + 1}\right)\frac{1}{n-1}$	$ln\left[\left(\frac{C_0}{C_t}\right)^{n-1} - 1\right] = -rt + lnA$	(5)	[36]
Wolborska	$\frac{C_t}{C_0} = e^{\frac{\beta C_0}{N_0}t - \frac{\beta Z}{U}}$	$ln\frac{C_t}{C_0} = \frac{\beta C_0}{N_0}t - \frac{\beta Z}{U}$	(6)	[39]
Modified dose-response	$\frac{C_t}{C_0} = 1 - \frac{1}{\left(\frac{C_0 Q t}{q_0 X}\right)^a + 1}$	$ln\left(\frac{C_t}{C_0 - C_t}\right) = aln(t) + aln\left(\frac{C_0 Q}{q_0 X}\right)$	(7)	[38]

3. Results and discussions

3.1. Effect of CDI technique on the MBC adsorption capability

The difference between the breakthrough curves of MBC with and without CDI was investigated in this study and the results are shown in Fig. 2, with the breakthrough curves for the first 6 h period depicted in the insert. The results presented in Fig. 2 indicate that the column length was shorter than the mass transfer zone (MTZ), resulting in a very small breakthrough time ($t_B \sim 0$). The MBC column reached the exhaustion time (t_E) at approximately 360 min. The introduction of CDI extended t_E by 12 fold to 4320 min. The values of t_B and t_E are normally determined based on the adsorbate concentration in the effluent. The time required for the adsorbate concentration in the effluent to reach 5% of its concentration in the influent is usually termed as the breakthrough time. The time needed for adsorbate concentration in the effluent to arrive at 95% of the influent concentration is called exhaustion time [5]. Due to the short column length, the t_B value was selected for a target removal of 90% as shown in the inset in Fig. 2. According to this criterion, the t_B for MBC and MBC-CDI columns were found to be 5 min and 60 min, respectively. When the adsorption removal dropped to 10%, the time corresponding to this value was considered as t_E for the two treatments. The reason for choosing 10% removal as a mark for bed exhaustion is that the adsorption capacity of MBC bed started to decrease slightly after this removal level (<10% change after 360 min of column operation). The phenomenon of adsorbent not being able to reach 100% exhaustion was explained by the possibility of adsorbate reaction with other materials on adsorbent where the latter serves as a catalyst [31]. Given that nitrate solution was prepared with distilled water, the only possibility left for speculation is the presence of some materials on MBC that were not washed off when cleaning was applied. These materials might have reacted with nitrate. We conducted FTIR analysis in our previous work [20] and observe that the signal intensity of functional groups reduced after nitrate adsorption indicating nitrate involvement in chemical reactions.

Although CDI increased the t_E, it did not affect t_B. CDI might have improved mass transfer of nitrate through film, pore and surface diffusion mechanisms by boosting electrostatic interactions (e.g. Columbia attraction [40]), which is deemed to be one of the major adsorption mechanisms of nitrate onto BC [41]. However, with the short column length and the influent flowrate applied, this effect was not sufficient to slow down the movement of MTZ with respect to the solution flow to achieve a typical *S-shape* breakthrough curve. Practically, t_B is linked to the set removal target of contaminants which is not necessary 100% in real life applications.

The common NO_3^- removal mechanisms using BC alone are functional groups and ion exchange mechanisms and to a lesser extent the physical adsorption which is highly influenced by micro-pore volumes and surface area [42,43]. It is likely that the electrostatic interaction mechanisms are also involved in the removal in this study as electro-sorption capacity increases with increasing thermal pyrolysis temperature of the biomass material. High temperatures lead to higher graphitization levels, minimizes the electrical resistance of the MBC surface and increases the specific surface area [44]. In terms of removal mechanisms, the case with CDI can be slightly different as the electrostatic interaction is the prominent mechanism. The capacitance of the CDI electrodes is limited; however, a large surface area of MBC enhances the removal efficiency when combined with CDI. High surface area and good mass transfer were the key points for better adsorption and electrocatalysis applications [48], which can explain a higher removal for CDI with MBC compared with the latter alone. The high surface area and porous structure of MBC are demonstrated in the SEM micrograph (Fig. S-1a). The graphitization of MBC that supports the electrical effects of CDI is shown in the XRD diffractogram depicted in Fig. S-1b. The degree of crystallization as an indicator for the graphitization of MBC was calculated to be 20.72%.

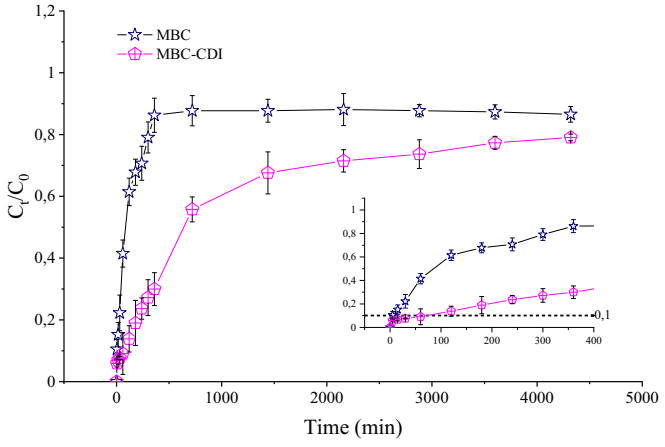

Fig. 2. Nitrate relative concentration variation with time for MBC alone and combined with CDI.

Testing an integrated electrochemical (EC)-adsorption system was addressed by a limited number of studies. Most of the studies used biochar as a material for manufacturing CDI electrodes. For instance, Dehkhoda et al. and Maniscalco et al. [45,46] examined the removal efficiency of NaCl with CDI electrodes manufactured from BC made from wood and almond shells. They both found that the pore structure of biochar plays an important role in electro-sorption processes. A recent study performed by Stephanie et al. [47] reported an improvement in electro-sorption based CDI of NaCl by customizing the surface chemistry of BC with the addition of an amine group. Compared to the studies mentioned above, the authors could only find one study with a similar experimental configuration to the one applied in this study (i.e. integrated CDI electrode into biochar column). However, this study used ion exchange resin beads as dispersed adsorbents inside a stainless-steel sieve serving as an anode and a copper plate as a cathode [48]. It was found that the synergistic effect of both adsorption and EC resulted in nitrate removal equal to the combination of the removal of the two processes individually.

Two commonly applied criteria in fixed-bed studies were applied to quantify the effect of integrating CDI into the MBC column on the system's overall performance. These are specific throughput and carbon usage rates (CUR) that were calculated for MBC and MBC-CDI systems using Eqs. (8)–(10) [40]:

$$\text{Specific throughput} = \frac{t_B}{EBTC\ \rho_B} \tag{8}$$

$$EBTC = \frac{V_B}{Q} \tag{9}$$

$$CUR = \frac{1}{\text{Specific throughput}} \tag{10}$$

when applying these t_B values in Eqs. (8)–(10), it was found that CDI-MBC had more than 10 times higher specific throughput compared to MBC, which in turn results in 10-time lower CUR, as it can be seen in Fig. 3.

3.2. Application of fixed-bed sorption models

The fixed bed sorption models (non-linear format) presented in Table 1 were fitted against the experimental BTC data for MBC and MBC-CDI columns. The results are presented in Figs. 4 and 5, respectively. It can be seen from both figures that Thomas and Wolborska models did not provide a good fitting for the experimental data. The former predicted no change in relative concentration with time, while the latter predicted the change in relative concentration with time to be

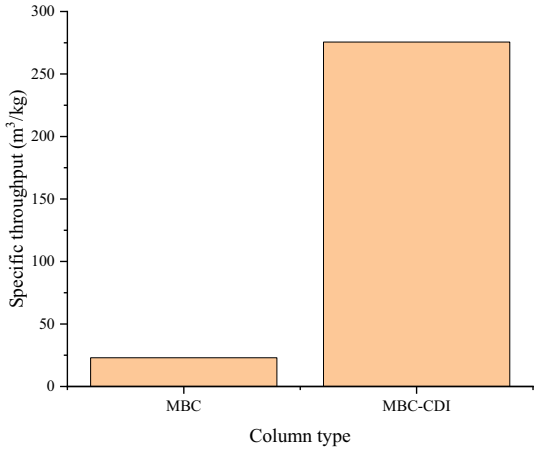

Fig. 3. Specific throughput for MBC and MBC-CDI columns.

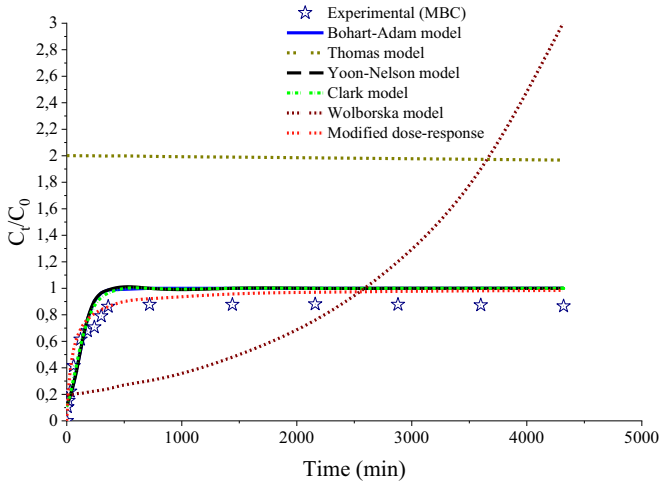

Fig. 4. Fitting of sorption models for MBC column.

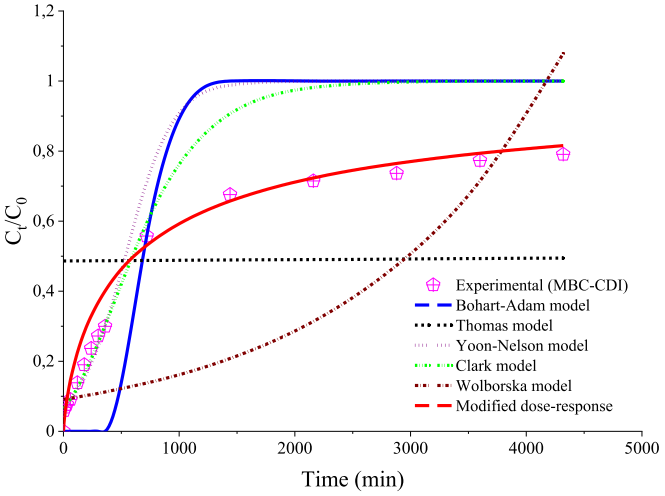

Fig. 5. Fitting of sorption models for MBC-CDI.

exponential. A study conducted by Lee et al. [29] on phosphate adsorption onto fixed-bed columns also found that Wolborska predicted exponential growth of relative concentration with time. Other models showed good agreement with the experimental data. Hence, further discussions of the models' parameters and their goodness of fit indicators will exclude Thomas and Wolborska models.

Tables 2–5 present the results of the fitting excises of the models with good agreement with the experimental data. It can be seen that the modified dose-response model provided the best fit for the experimental data of both columns with the highest R^2 and lowest χ^2 and *SSE*. Other models provided a decent fit for the experimental data and predicted well the adsorption parameters. For instance, the Yoon-Nelson model predicted well the value of τ for both columns. Similarly, the Bohart-Adam model predicted a higher sorption capacity of MBC-CDI than MBC, which is reflected in the increased saturation time in the breakthrough curves. The Bohart-Adam model provided a good prediction for the first part of the breakthrough curve. The deviation from the experimental data starts to grow bigger as the columns reach saturation. Other studies reported a similar trend on nitrate adsorption onto the fixed-bed column of activated carbon [49,50].

The models' parameters provide useful information for the characteristics of the two columns. Reflecting on the fitting results for the fixed bed models, it seems that incorporating CDI improved the rates for mass transfer and the possible reactions of nitrate with MBC indicated by the increase in Bohart-Adam rate constant. This is also evident in the increase in r parameter for Clark model that is derived from the mass transfer coefficient [36]. CDI also increased the adsorption capacity of MBC column, which is seen in the significant increase in the parameters representing maximum adsorption capacity in Bohart Adams and modified dose response models (q_0 and N_0).

It is noteworthy that the linear format of the fixed-bed sorption models was also fitted against the BTC experimental data in this study. It was found that the linear format of all the models except modified dose-response produced poor fittings represented by low R^2 and high χ^2 and *SSE* (results are presented in Supplementary materials, Sections 2–5). All in all, it can be concluded that any of the four models, Bohart-Adam, Yoon-Nelson, Clark, or modified dose-response in their non-linear format, can adequately predict breakthrough curves of nitrate adsorption onto MBC and MBC-CDI. However, the modified dose-response model is the best model for predicting the breakthrough curve behaviour of MBC and MBC-CDI.

3.3. Degaussing versus backflush alone with TW and DW

The ability of an adsorbent to regeneration is an important environmental and economical aspect that determines its feasibility for water decontamination [51,52]. In this study, the regeneration of the saturated column was conducted using the simplest means for this purpose represented by applying DW and TW. The elution curves of both water types for two cycles are presented in Fig. 6a and b, respectively. These curves resemble the typical elution curve for the fixed-bed desorption process presented by Worch [57]. It should be mentioned that the letter C in the legend for this figure and the following elution curves' figures denotes the regeneration cycle. The concentration of desorbed adsorbate reaches a maximum at the first quarter of the elution time and then tails off as the elution time goes on.

DW resulted in better desorption compared to TW. This is due to the stronger stripping capacity of deionized water that does not contain any element to compete with nitrate. DW water recovered a maximum of 7,4 mg/L and 5,6 mg/L in the first and second cycles. In comparison, TW resulted in a maximum nitrate desorbed of 5,3 mg/L for cycle 1 and

Table 2
Bohart-Adam model fitting parameters.

Column type	Model parameters		Fitness parameters		
	k_{BA}	N_0	R^2	χ^2	*SSE*
MBC	0,0012	48,64	0,899	0,280	0,227
MBC-CDI	0,0040	290,58	0,808	4430	0,648

Table 3
Yoon-Nelson model fitting parameters.

Column type	Model parameters		Fitness parameters		
	k_{YN}	τ	R^2	χ^2	*SSE*
MBC	0,018	112,68	0,899	0,400	0,227
MBC-CDI	0,005	533,61	0,861	0,476	0,377

Table 4
Clark model fitting parameters.

Column type	Model parameters			Fitness parameters		
	A	*r*	*n*	R^2	χ^2	*SSE*
MBC	0,015	0,011	1007	0,920	0,302	0,177
MBC-CDI	0,019	0,013	1007	0,883	0,373	0,295

Table 5
Modified dose-response model fitting parameters.

Column type	Model parameters		Fitness parameters		
	a	q_o	R^2	χ^2	*SSE*
MBC	0,927	70,11	0,927	0,218	0,127
MBC-CDI	0,761	849,28	0,960	0,216	0,051

decreased to 4,3 mg/L for cycle 2. To quantify the efficiency of the regeneration process, the concentration factor defined as the maximum eluent concentration divided by the influent concentration was calculated for both elution solutions [53]. The concentration factor for DW was calculated to be 0,49 and 0,37 for cycles 1 and 2, respectively. The corresponding figures of concentration factor for TW were lower (0,35 and 0,28 for cycles 1 and 2, respectively). The concentration factors obtained from DW and TW are several folds lower than those reported in other studies [52,53]. This is due to the use of chemicals such as EDTA-Na_2 and HNO_3 by the studies mentioned above in the regeneration process. Nitrate desorption from biochar has been attributed to low bond energy and ion exchange mechanisms [42]. In the case of this study, the low bond energy and the concentration difference between elution solution and biochar surface had the main role in desorbing nitrate.

The results of adsorption and desorption experiments suggest that the adsorption of nitrate onto MBC is a faster process than desorption. This might be an attractive trait for MBC in soil amendment applications, but it may be regarded as a disadvantage for MBC in filtration applications. Hence, exploring ways of speeding up the regeneration and nitrate recovery from MBC is important. This study proposes using degaussing coupled with the backflush for regeneration and nitrate recovery.

Fig. 7 presents a comparison between nitrate recoveries of degaussing coupled with DW backflush for three cycles. An extra cycle more than the DW and TW was conducted to monitor the impact of the cycles' number on regeneration efficiency with degaussing, given it is of special interest in this study. It can be seen that applying degaussing on the saturated column resulted in a very similar unsymmetrical shape to the elution curves obtained with DW and TW, with a rapid nitrate concentration increase for the first 30 min, followed by a flatter diminution as shown in Figs. 6 and 7. The maximum effluent of nitrate concentration peak was achieved in about 30 min for all the cycles. About 73% nitrate recovery was achieved for the first cycle with an elution concentration of 11 mg/L. For DW alone, the maximum elution concentration was about 7,5 mg/L, approximately 50% nitrate recovery. The degaussing resulted in a further increase in eluted nitrate by 23%. The first cycle of degaussing and DW backflush resulted in approximately double the amount of nitrate eluted obtained with TW. For the second and third cycles, the released nitrate concentration became lower at 9 and 7 mg/L, respectively. Similar to DW and TW, the maximum eluted nitrate decreased by about 2 mg/L after each cycle. So, degaussing did not influence the effect of cycles numbers on the loss of desorption capacity. As the desorption time went on to 6 h, the eluted nitrate concentration dropped significantly to 2,5, 1,8 and 1,3 mg/L for cycles 1, 2 and 3, respectively. This drop was lower than the drop recorded with TW and DW. This suggests that the best application for degaussing is for a short

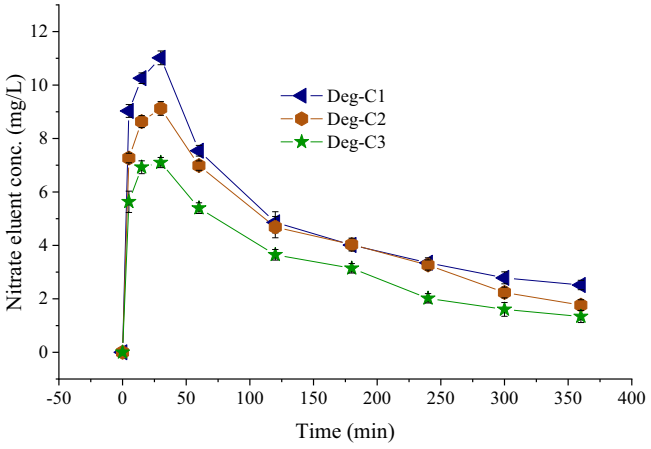

Fig. 7. Nitrate desorption with degaussing for 3 cycles.

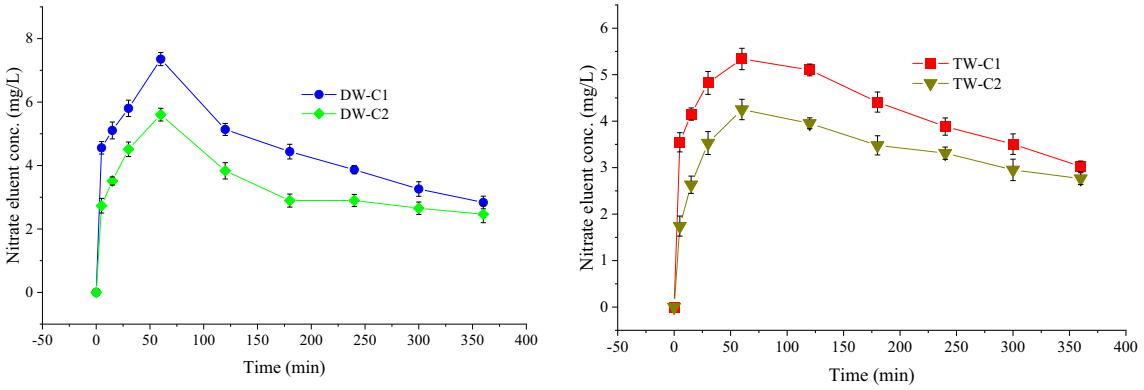

Fig. 6. Nitrate desorption with DW (a) and TW (b).

elution time (the first hour); then, the effect becomes negligible or even negative at a long elution time. Although a limited number of cycles were performed in this study, one can conveniently infer that desorption with degaussing drops almost consistently with cycles at least for the three cycles performed (Maximum desorption drop by about 2 mg/L per cycle). To get more insight into the potential cyclic degradation effects on degaussing performance, a larger number of cycles should be applied, and this can be explored in future studies.

To check if faradic reactions have taken place during the degaussing, FTIR analysis were conducted for virgin and degaussed MBC samples and the results are presented in Fig. S-6. The FTIR spectra for both samples were almost identical suggesting that applied electrical energy for degaussing was not high enough to induce such reactions. Faradic reactions are known to cause some chemical changes in the surface functional groups of adsorbents such as the formation of -OH and -COOH [54]. Carboxylic and hydroxyl groups have FTIR peaks around 1700 cm^{-1} and 3400 cm^{-1} [55], and the spectra for both samples were the same in these regions. There was only small changes noticed in the MBC spectra after regeneration with degaussing around 1000 cm^{-1} and 1500 cm^{-1}, and these are likely to be related to the remnant nitrate on the char [56].

The mechanisms through which degaussing improved the desorption of nitration from MBC can be explained by the effect of the generated magnetic field on the interaction of nitrate molecules with biochar. It was stated the magnetic field could affect materials interactions through coulomb energy and electron spin selection rules [57]. Coulombic interactions (repulsion and attraction) are the strongest interactions between adsorbates and adsorbents [40]. It was found that the application of a magnetic field led to a decrease in the adsorption of Ba^{+2} onto zeolite [58,59]. This diminution was attributed to the weakening of the aqueous solution's hydrogen bonds upon exposure to a magnetic field; consequently, the hydration shell of the ions increases. The increase in the hydration shell can increase the water molecules' cohesion forces with the nitrate ions, stripping them off of the biochar particles. This effect can be more pronounced in ions with high hydration numbers, such as nitrate, with 64 [60]. The effect of the magnetic field on the hydration of ions was found to diminish with time, which could explain the significant drop in nitrate elution concentration with degaussing. The effect of degaussing on the desorption of nitrate can also be explained by the magnetic properties of nitrate ions tested in this study. Omar et al. [61] explained in their study that the sensitivity of ions to a magnetic field is attributed to their magnetic susceptibility. The magnitude and the sign of the magnetic susceptibility determine the nature of their reaction to the magnetic field. A positive value of the magnetic susceptibility indicates that the ion favours the applied magnetic field, whereas a negative value indicates a repulsive response of the ion to the applied magnetic field. It was reported that sodium nitrate has a magnetic susceptibility of $-25{,}6 \times 10^{-6}$ cm^3/mol [62]. This might have contributed to the repulsion of nitrate to the generated magnetic field, which consequently induced the desorption of nitrate.

3.4. Nitrate removal with regenerated filter

After the completion of desorption tests, the reusability of the filter for nitrate removal was examined. Fig. 8 presents nitrate adsorption comparison between fresh MBC, MBC-CDI and MBC-CDI with regenerated bed with degaussing and DW backflush for two cycles. The use of CDI with the regenerated beds even for the second cycle provided better nitrate adsorption than MBC alone. This proves the effectiveness of CDI and degaussing in improving the adsorption/desorption of biochar. It seems that the regeneration of the bed did not affect t_E for the MBC-CDI process as both fresh and regenerated beds had similar t_E. The most pronounced nitrate concentration variation can be observed in the first 6 h (insert of Fig. 7). After this, the difference in concentration variation between fresh and regenerated MBC-CDI got smaller. The adsorption capacity of nitrate after 6 h of adsorption was calculated for all bed types

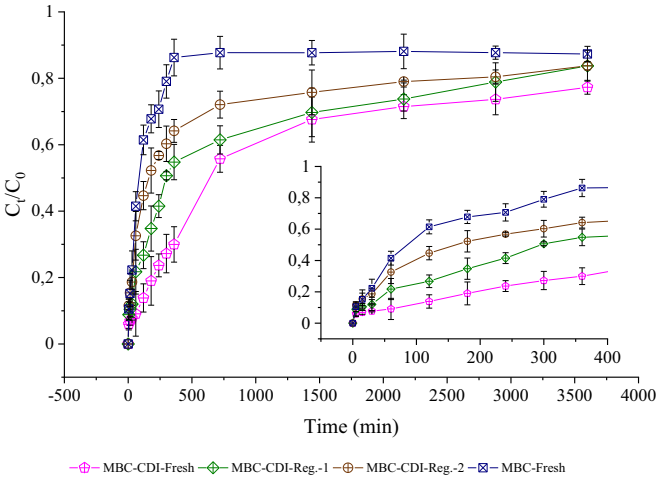

Fig. 8. Comparison of nitrate relative concentration variation with time of MBC-CDI for fresh and regenerated columns.

(fresh and regenerated) using Eq. (1). It was found that the MBC had a q value of 0,89 mg/g, while the corresponding value for MBC-CDI-Fresh, MBC-CDI-Reg.1 and MBC-CDI-Reg.2 were 4,50 mg/g, 2,94 mg/g and 2,33 mg/g, respectively. So, the adsorption capacity of fresh and regenerated MBC-CDI was 2,5–5 higher than that of fresh MBC.

The majority of studies conducted on reusability of regenerated adsorbents focused on testing the adsorption efficiency at a fixed adsorption time, mostly at the equilibrium point. This study looked at the breakthrough curves of the regenerated beds as opposed to fresh beds. Nitrate removal efficiency varied throughout the time of adsorption experiments. As stated above, the different beds' removal efficiency in Fig. 8 varied significantly in the first 6 h. Then the difference decreased toward the end of the adsorption experiments. After 60 h of adsorption time, the nitrate removal difference between cycles 1 and 2 was none. Similar to our results, Afjeh et al. [63] found that the regeneration of hydrogel rice husk biochar resulted in the same adsorption in the first two cycles. The specific throughput and CUR of the regenerated beds were calculated for 90% nitrate removal. The first regeneration cycle resulted in a specific throughput of 68,90 m^3/kg and CUR of 0,14 kg/m^3. These values are about three times higher than that of the fresh MBC. In comparison, the second cycle of regeneration resulted in the same specific throughput and CUR as that of fresh MBC. This highlights the significant improvement CDI and degaussing had on the adsorption/desorption capacity of MBC.

The similarity of the degaussing breakthrough and desorption curves with that of fresh and regenerated MBC with TW and DW suggests that the applied electrical energy during degaussing only improved nitrate desorption and did not alter its interaction with MBC. The change in nitrate chemistry upon exposure to electrical power was also unlikely to occur as nitrite (being an intermediate for nitrate conversion to other nitrogen forms) was not detected in the ion chromatography measurements. In addition, the applied voltage was a relatively high frequency compared to the DC applied in the CDI system there may not have been time for any chemical or water based physical reactions to occur, as there was no evidence of hydrogen production or other gaseous outputs during degaussing. With regards to MBC degradation, it is an extremely stable physical form, effectively an activated carbon and is commonly used as an inert electrode at hundreds of volts and is not subject to fast degradation unless arcing is involved (as in plasma arc decomposition systems) or if heated beyond 1000 °C. Mechanical vibration may cause wear, however this is a slow process if flows are kept to a reasonable level.

4. Energy considerations with CDI and degaussing cycles

One of the important research questions for newly developed techniques is the estimation for energy and cost requirement and how do they gauge against competing technologies. With regards to the proposed technique in this study, we can identify the competing technologies and establish comparison between our system and these technologies when applicable. Since this technology incorporates CDI and degaussing concepts for adsorption/desorption of biochar, the comparison can be made with either CDI and its regeneration techniques or biochar adsorption enhancement techniques (mainly impregnation with metals) and common desorption methods (chemical and thermal).

The power used at any instant in the sorption phase is simply the DC voltage applied multiplied by the current drawn. In order to calculate the total energy consumed the power can be integrated over the application period to get Whrs were 1Whr is 3.6 kJ. As the applied cell voltage was held constant, the average power figure can be achieved by logging the DC current drawn over time, taking its average and multiplying this value by the constant applied voltage i.e. $P_{CDI(mean)} = I_{DC(mean)} \times V_{DC}$. To calculate the consumed energy for the CDI sorption period, the average power figure P_{CDI} can be multiplied by the CDI application time to get the consumed energy in Joules. i.e. $P_{CDI(mean)} \times t_{CDI}$. Based on this approach the total energy spent during the adsorption cycle was calculated to be 82,1 J. The profile of the current drawn during the adsorption cycle was recorded and the results are shown in Fig. 9. The charge efficiency of the MBC-CDI system was determined using Eq. (11) [64,65]. The calculated charge efficiency for our system was 78,6%. The achieved charge efficiency in this study was slightly higher than that reported in [64] for CDI removal of NaCl at the same applied voltage.

$$\Lambda = \frac{(C_0 - C_t)vF}{\int Idt} \times 100\% \tag{11}$$

Unlike the CDI sorption phase, the degaussing applied is a square AC waveform at 100 Hz. For non-sinusoidal waveforms the easiest and most common approach is to multiply the current and voltage waveforms point by point and average over a cycle to obtain the average power per cycle. This approach is commonly used by high accuracy so-called smart energy meters for billing purposes. In both the CDI sorption and degaussing cycles we used a high precision, true rms, digital multimeter namely a Fluke model 289, to measure the voltage and current components as applicable. For the CDI sorption cycle DC voltage and current, and for the degaussing cycle applied AC voltage and current, as well as any discharge DC current from the CDI cell (seen as a negative current flow in Fig. 10).

To capture the waveforms, we used a Tektronix TP2014 oscilloscope with P6021 current probe, 10A, 100 MHz. The captured waveforms were analyzed with Tektronix Wavestar software (Fig. S-7). The figure shows the change in current waveform from the start of degaussing until

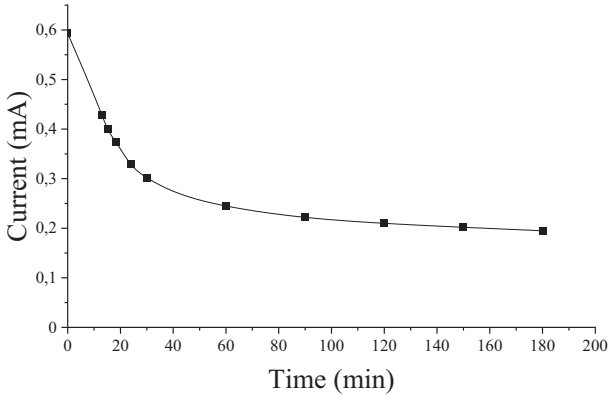

Fig. 9. CDI current profile for DC applied voltage of 1,2 V.

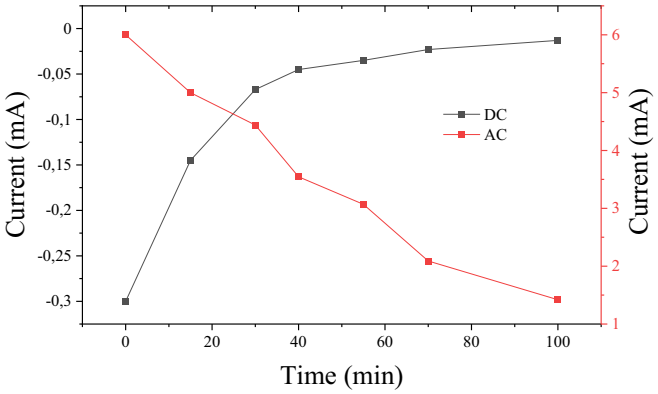

Fig. 10. Degaussing current profile for AC and DC components.

the end. To calculate the energy consumed for nitrate desorption, Eq. (12) [66] was applied. The energy consumed during degaussing was calculated to be 43,7 J/mmol of nitrate. Similar energy figure was reported by Zhou et al. [66] who tested an approach somewhat similar to ours using alternating field for regenerating CDI electrodes.

$$E = \frac{\int uIdt}{C_d V} \tag{12}$$

Importantly by simply monitoring the DC current it can be seen when the CDI bed has been regenerated marked by the discharge of the bed to ≈0 current in Fig. 10. Similarly the current drawn during the CDI application can also be monitored and readily correlated to the saturation level of the CDI bed, hence once the current declines to a certain level regeneration can be triggered (Fig. 9).

Comparing the enhancement induced by CDI and degaussing with common biochar improvement techniques is hard. Normally, improvement of biochar adsorption capacity of targeted pollutants is conducted by either activation with gases, steam or by modifying biochar with active elements and functional groups [67,68]. The source of energy and cost consumption in these techniques varies vastly as some involve the use of high temperatures while other use complex process or expensive and dangerous chemicals. In addition, it is important to highlight that this work reports on proof of concept, and the technique still requires thorough optimization for the operating parameters and design. Such an optimization step would help in determining the best conditions for the desirable outcome. Once this is done, one can fairly compare this technique with competing technologies.

5. Conclusions and future work

The effect of CDI integration into biochar (MBC) column adsorption on contaminants removal efficiency was investigated in this study. Nitrate was selected as a model contaminant due to its role in contaminating surface water, especially runoff events. Nitrate recovery and bed column regeneration was evaluated with a newly proposed approach of degaussing and compared with conventional regeneration methods with deionized and tap water. The breakthrough curves of MBC and MBC-CDI were analyzed using common fixed-bed column models. The adsorption efficiency of the fresh and regenerated column was evaluated using industrial known criteria such as specific throughput and CUR.

It was found that integrating CDI into the MBC column could extend the saturation time of the column by 12 folds. It also resulted in significantly higher specific throughput and lower CUR compared to MBC alone. The analysis of the breakthrough curves showed that the non-linear form Bohar-Adam, Clark, Yoon-Nelson and modified dose-response models could sufficiently predict the parameters of the adsorption process with MBC and MBC-CDI. However, the modified dose-response model exhibited the best goodness of fit to the

experimental data for both none-liner and linear forms of the models.

Applying degaussing along with deionized water backwash significantly improved the desorption of nitrate. Nevertheless, this improvement was only valid for the first 60 min; then nitrate desorption was the same or lower than that observed with conventional backwash with deionized water and tap water. Hence, this study recommends applying degaussing for a short time to get the best outcome of desorption. Nitrate adsorption efficiency of regenerated bed with degaussing and DW was used with CDI for nitrate adsorption and was better than MBC for two cycles. The specific throughput of the regenerated bed for the first cycle was higher than fresh MBC by about three fold for 90% nitrate removal. However, the regenerated bed for the second cycle had the same specific throughput and CUR as that of fresh MBC for the same nitrate target removal.

The energy consumption of CDI and degaussing was estimated a standard electrical perspective. The total energy consumed for the adsorption cycle was calculated to be 82,1 J. The charge efficiency of CDI and degaussing energy consumption were 78,6% and 43,7 J/mmol of NO_3^-, respectively. These figures were slightly better than the reported values I the literature.

The positive outcome obtained in this study using CDI and degaussing and chemical-free approaches for improving adsorption of biochar encourages further research in this area with different model contaminants, sample matrix, feedstocks and pyrolysis conditions. It is also beneficial to optimize the design and operation of the system to achieve the best performance of adsorption and desorption processes in future studies.

Nomenclature

A	Clark model constant (−)
a	Modified dose-response model constant (−)
C_0	Influent adsorbate concentration ($mg{\cdot}L^{-1}$)
C_t	Effluent adsorbate concentration ($mg{\cdot}L^{-1}$)
E	Desorption energy (J/mmol)
F	Faraday constant 96.485 ($C{\cdot}mol^{-1}$)
I	Electrical current (mA)
k_{BA}	Bohart-Adam rate constant ($L{\cdot}mg^{-1}{\cdot}min^{-1}$)
k_T	Thomas rate constant ($L{\cdot}mg^{-1}{\cdot}min^{-1}$)
k_{YN}	Yoon-Nelson rate constant (min^{-1})
N_0	Maximum sorption capacity of adsorbent per unit volume of bed ($mg{\cdot}L^{-1}$)
n	Freundlich constant (−)
Q	Column flow rate ($L{\cdot}min^{-1}$)
q_0	Maximum adsorption capacity per unit mass of adsorbent ($mg{\cdot}g^{-1}$)
r	Clark model constant (min^{-1})
t	Sorption time (min)
U	Column superficial velocity ($cm{\cdot}min^{-1}$)
u	Applied voltage during desorption (V)
V	Solution volume (L)
V_B	Bed volume including porosity (m^3)
X	Adsorbent mass (g)
Z	Bed depth (cm)

Greek letters

β	Mass transfer constant of Wolbroska model (min^{-1})
Λ	Charge efficiency (−)
τ	Time required for 50% adsorbate breakthrough
ρ_B	Bed density (kg/m^3), $\rho_{B=\ X/}V_B$

Declaration of competing interest

The authors declare that they have no known competing financial interests or personal relationships that could have appeared to influence the work reported in this paper.

Appendix A. Supplementary data

Supplementary data to this article can be found online at https://doi.org/10.1016/j.jwpe.2022.102786.

References

[1] E. Boyle, Nitrogen pollution knows no bounds, Science 356 (2017) 700–701, https://doi.org/10.1126/science.aan3242.

[2] H. Zhang, X. Kang, X. Wang, J. Zhang, G. Chen, Quantitative identification of nitrate sources in the surface runoff of three dominant forest types in subtropical China based on bayesian model, Sci. Total Environ. 703 (2020), 135074, https://doi.org/10.1016/j.scitotenv.2019.135074.

[3] Z.-H. Wang, S.-X. Li, Chapter three - nitrate N loss by leaching and surface runoff in agricultural land: a global issue (a review), in: D.L. Sparks (Ed.), Advances in Agronomy, Academic Press, 2019, pp. 159–217, https://doi.org/10.1016/bs.agron.2019.01.007.

[4] D.C. Bouchard, M.K. Williams, R.Y. Surampalli, Nitrate contamination of groundwater: sources and potential health effects, J. AWWA 84 (1992) 85–90, https://doi.org/10.1002/j.1551-8833.1992.tb07430.x.

[5] X. Xu, B. Gao, X. Tan, X. Zhang, Q. Yue, Y. Wang, Q. Li, Nitrate adsorption by stratified wheat straw resin in lab-scale columns, Chem. Eng. J. 226 (2013) 1–6.

[6] J. Yang, H. Li, D. Zhang, M. Wu, B. Pan, Limited role of biochars in nitrogen fixation through nitrate adsorption, Sci. Total Environ. 592 (2017) 758–765, https://doi.org/10.1016/j.scitotenv.2016.10.182.

[7] M. Kalaruban, P. Loganathan, W.G. Shim, J. Kandasamy, H.H. Ngo, S. Vigneswaran, Enhanced removal of nitrate from water using amine-grafted agricultural wastes, Sci. Total Environ. 565 (2016) 503–510, https://doi.org/10.1016/j.scitotenv.2016.04.194.

[8] Z. Xu, Z. Wan, Y. Sun, X. Cao, D. Hou, D.S. Alessi, Y.S. Ok, D.C.W. Tsang, Unraveling iron speciation on fe-biochar with distinct arsenic removal mechanisms and depth distributions of as and fe, Chem. Eng. J. 425 (2021), 131489, https://doi.org/10.1016/j.cej.2021.131489.

[9] Y. Shi, R. Shan, L. Lu, H. Yuan, H. Jiang, Y. Zhang, Y. Chen, High-efficiency removal of Cr(VI) by modified biochar derived from glue residue, J. Clean. Prod. 254 (2020), 119935, https://doi.org/10.1016/j.jclepro.2019.119935.

[10] P. Krasucka, B. Pan, Y. Sik Ok, D. Mohan, B. Sarkar, P. Oleszczuk, Engineered biochar – a sustainable solution for the removal of antibiotics from water, Chem. Eng. J. 405 (2021), 126926, https://doi.org/10.1016/j.cej.2020.126926.

[11] S.S.A. Alkurdi, I. Herath, J. Bundschuh, R.A. Al-Juboori, M. Vithanage, D. Mohan, Biochar versus bone char for a sustainable inorganic arsenic mitigation in water: what needs to be done in future research? Environ. Int. 127 (2019) 52–69, https://doi.org/10.1016/j.envint.2019.03.012.

[12] P.R. Yaashikaa, P.S. Kumar, S. Varjani, A. Saravanan, A critical review on the biochar production techniques, characterization, stability and applications for circular bioeconomy, Biotechnol. Rep. 28 (2020), e00570, https://doi.org/10.1016/j.btre.2020.e00570.

[13] H.M. Jang, E. Kan, Engineered biochar from agricultural waste for removal of tetracycline in water, Bioresour. Technol. 284 (2019) 437–447, https://doi.org/10.1016/j.biortech.2019.03.131.

[14] M.C. Qhubu, L.G. Mgidlana, L.M. Madikizela, V.E. Pakade, Preparation, characterization and application of activated clay biochar composite for removal of Cr(VI) in water: isotherms, kinetics and thermodynamics, Mater. Chem. Phys. 260 (2021), 124165, https://doi.org/10.1016/j.matchemphys.2020.124165.

[15] S.L.B. Navarro, C.E.C. Rodrigues, Macadamia oil extraction methods and uses for the defatted meal byproduct, Trends Food Sci. Technol. 54 (2016) 148–154, https://doi.org/10.1016/j.tifs.2016.04.001.

[16] S. Wongcharee, V. Aravinthan, L. Erdei, Mesoporous activated carbon-zeolite composite prepared from waste macadamia nut shell and synthetic faujasite, Chin. J. Chem. Eng. 27 (2019) 226–236, https://doi.org/10.1016/j.cjche.2018.06.024.

[17] M.T. Dao, T.T.T. Nguyen, X.D. Nguyen, D.D. La, D.D. Nguyen, S.W. Chang, W. J. Chung, V.K. Nguyen, Toxic metal adsorption from aqueous solution by activated biochars produced from macadamia nutshell waste, Sustainability. 12 (2020) 7909, https://doi.org/10.3390/su12197909.

[18] M.R.B. Roser, Using Unique Carbon Source Combinations to Increase Nitrate and Phosphate Removal in Bioreactors, M.S, University of Minnesota, 2016, https://www.proquest.com/docview/1818523742/abstract/EDB02B7D5A134BF6PQ/1. (Accessed 17 September 2021).

[19] X. Yang, Z. Chen, Q. Wu, M. Xu, Enhanced phenanthrene degradation in river sediments using a combination of biochar and nitrate, Sci. Total Environ. 619–620 (2018) 600–605, https://doi.org/10.1016/j.scitotenv.2017.11.130.

[20] S. Bakly, R.A. Al-Juboori, L. Bowtell, Macadamia nutshell biochar for nitrate removal: effect of biochar preparation and process parameters, C—J. Carbon Res. 5 (2019) 47.

[21] F. Salvador, N. Martin-Sanchez, R. Sanchez-Hernandez, M.J. Sanchez-Montero, C. Izquierdo, Regeneration of carbonaceous adsorbents. Part II: chemical, microbiological and vacuum regeneration, Microporous Mesoporous Mater. 202 (2015) 277–296, https://doi.org/10.1016/j.micromeso.2014.08.019.

[22] T.J. Welgemoed, C.F. Schutte, Capacitive deionization TechnologyTM: an alternative desalination solution, Desalination 183 (2005) 327–340, https://doi.org/10.1016/j.desal.2005.02.054.

[23] K.Z. Huang, H.L. Tang, Temperature and desorption mode matter in capacitive deionization process for water desalination, Environ. Technol. 41 (2020) 3456–3463, https://doi.org/10.1080/09593330.2019.1611941.
[24] Q. Yao, H.L. Tang, Occurrence of re-adsorption in desorption cycles of capacitive deionization, J. Ind. Eng. Chem. 34 (2016) 180–185, https://doi.org/10.1016/j.jiec.2015.11.004.
[25] Q. Yao, H.L. Tang, Effect of desorption methods on electrode regeneration performance of capacitive deionization, J. Environ. Eng. 143 (2017) 04017047, https://doi.org/10.1061/(ASCE)EE.1943-7870.0001245.
[26] K. AlAmeri, A. Giwa, L. Yousef, A. Alraeesi, H. Taher, Sorption and removal of crude oil spills from seawater using peat-derived biochar: an optimization study, J. Environ. Manag. 250 (2019), 109465, https://doi.org/10.1016/j.jenvman.2019.109465.
[27] J. He, A. Cui, S. Deng, J.P. Chen, Treatment of methylene blue containing wastewater by a cost-effective micro-scale biochar/polysulfone mixed matrix hollow fiber membrane: performance and mechanism studies, J. Colloid Interface Sci. 512 (2018) 190–197, https://doi.org/10.1016/j.jcis.2017.09.106.
[28] E.W. Rice, R.B. Baird, A.D. Eaton, L.S. Clesceri, Standard Methods for the Examination of Water and Wastewater, 23rd ed., American Public Health Association, Washington, DC, 2017.
[29] C.-G. Lee, J.-H. Kim, J.-K. Kang, S.-B. Kim, S.-J. Park, S.-H. Lee, J.-W. Choi, Comparative analysis of fixed-bed sorption models using phosphate breakthrough curves in slag filter media, Desalin. Water Treat. 55 (2015) 1795–1805.
[30] O. Hamdaoui, Removal of copper (II) from aqueous phase by purolite C100-MB cation exchange resin in fixed bed columns: modeling, J. Hazard. Mater. 161 (2009) 737–746.
[31] G.S. Bohart, E.Q. Adams, Some aspects of the behavior of charcoal with respect to chlorine, J. Am. Chem. Soc. 42 (1920) 523–544.
[32] H.C. Thomas, Heterogeneous ion exchange in a flowing system, J. Am. Chem. Soc. 66 (1944) 1664–1666.
[33] H.C. Thomas, Chromatography: a problem in kinetics, Ann. N. Y. Acad. Sci. 49 (1948) 161–182.
[34] Y.H. Yoon, J.H. Nelson, Application of gas adsorption kinetics I. A theoretical model for respirator cartridge service life, Am. Ind. Hyg. Assoc. J. 45 (1984) 509–516.
[35] Z. Aksu, F. Gönen, Biosorption of phenol by immobilized activated sludge in a continuous packed bed: prediction of breakthrough curves, Process Biochem. 39 (2004) 599–613.
[36] R.M. Clark, Evaluating the cost and performance of field-scale granular activated carbon systems, Environmental Science & Technology. 21 (1987) 573–580.
[37] O. Hamdaoui, Dynamic sorption of methylene blue by cedar sawdust and crushed brick in fixed bed columns, J. Hazard. Mater. 138 (2006) 293–303.
[38] G. Yan, T. Viraraghavan, M. Chen, A new model for heavy metal removal in a biosorption column, Adsorp. Sci. Technol. 19 (2001) 25–43.
[39] A. Wolborska, Adsorption on activated carbon of p-nitrophenol from aqueous solution, Water Res. 23 (1989) 85–91.
[40] J.C. Crittenden, R.R. Trussell, D.W. Hand, K. Howe, G. Tchobanoglous, MWH's Water Treatment: Principles and Design, John Wiley & Sons, 2012.
[41] R.B. Fidel, D.A. Laird, K.A. Spokas, Sorption of ammonium and nitrate to biochars is electrostatic and pH-dependent, Sci. Rep. 8 (2018) 1–10.
[42] R. Chintala, J. Mollinedo, T.E. Schumacher, S.K. Papiernik, D.D. Malo, D.E. Clay, S. Kumar, D.W. Gulbrandson, Nitrate sorption and desorption in biochars from fast pyrolysis, Microporous Mesoporous Mater. 179 (2013) 250–257.
[43] K. Kameyama, T. Miyamoto, T. Shiono, Y. Shinogi, Influence of sugarcane bagasse-derived biochar application on nitrate leaching in calcaric dark red soil, J. Environ. Qual. 41 (2012) 1131–1137.
[44] C. Banik, M. Lawrinenko, S. Bakshi, D.A. Laird, Impact of pyrolysis temperature and feedstock on surface charge and functional group chemistry of biochars, J. Environ. Qual. 47 (2018) 452–461.
[45] A.M. Dehkhoda, N. Ellis, E. Gyenge, Effect of activated biochar porous structure on the capacitive deionization of NaCl and ZnCl2 solutions, Microporous Mesoporous Mater. 224 (2016) 217–228.
[46] M.P. Maniscalco, C. Corrado, R. Volpe, A. Messineo, Evaluation of the optimal activation parameters for almond shell bio-char production for capacitive deionization, Bioresour. Technol. Rep. 11 (2020) 100435.
[47] H. Stephanie, T.E. Mlsna, D.O. Wipf, Functionalized biochar electrodes for asymmetrical capacitive deionization, Desalination 516 (2021) 115240.
[48] M. Kalaruban, P. Loganathan, J. Kandasamy, R. Naidu, S. Vigneswaran, Enhanced removal of nitrate in an integrated electrochemical-adsorption system, Sep. Purif. Technol. 189 (2017) 260–266.
[49] S. Najmi, M.S. Hatamipour, P. Sadeh, I. Najafipour, F. Mehranfar, Activated carbon produced from Glycyrrhiza glabra residue for the adsorption of nitrate and phosphate: batch and fixed-bed column studies, SN Appl. Sci. 2 (2020) 1–22.
[50] R. Gouran-Orimi, B. Mirzayi, A. Nematollahzadeh, A. Tardast, Competitive adsorption of nitrate in fixed-bed column packed with bio-inspired polydopamine coated zeolite, journal of environmental, Chem. Eng. 6 (2018) 2232–2240.
[51] S. Biswas, U. Mishra, Continuous fixed-bed column study and adsorption modeling: removal of lead ion from aqueous solution by charcoal originated from chemical carbonization of rubber wood sawdust, J. Chem. 2015 (2015), e907379, https://doi.org/10.1155/2015/907379.
[52] C.B. Lopes, E. Pereira, Z. Lin, P. Pato, M. Otero, C.M. Silva, J. Rocha, A.C. Duarte, Fixed-bed removal of Hg2+ from contaminated water by microporous titanosilicate ETS-4: experimental and theoretical breakthrough curves, Microporous Mesoporous Mater. 145 (2011) 32–40.
[53] P. Lodeiro, R. Herrero, M.E. Sastre de Vicente, Batch desorption studies and multiple sorption–regeneration cycles in a fixed-bed column for Cd(II) elimination by protonated Sargassum muticum, J. Hazard. Mater. 137 (2006) 1649–1655, https://doi.org/10.1016/j.jhazmat.2006.05.003.
[54] A. Giurg, K. Denk, T. Bystron, M. Paidar, K. Bouzek, Electrode degradation mechanisms in capacitive deionisation, Desalination 497 (2021), 114622, https://doi.org/10.1016/j.desal.2020.114622.
[55] K. Zhang, P. Sun, Y. Zhang, Decontamination of Cr(VI) facilitated formation of persistent free radicals on rice husk derived biochar, Front. Environ. Sci. Eng. 13 (2019) 22, https://doi.org/10.1007/s11783-019-1106-7.
[56] H. Zhao, Y. Xue, L. Long, X. Hu, Adsorption of nitrate onto biochar derived from agricultural residuals, Water Sci. Technol. 77 (2017) 548–554, https://doi.org/10.2166/wst.2017.568.
[57] A. Buchachenko, R.G. Lawler, New possibilities for magnetic control of chemical and biochemical reactions, Acc. Chem. Res. 50 (2017), https://doi.org/10.1021/acs.accounts.6b00608.
[58] B.A. Baran, Influence of magnetic fields on adsorption and ion exchange from aqueous solutions, Adsorpt. Sci. Technol. 19 (2001), https://doi.org/10.1260/0263617011493999.
[59] K. Higashitani, J. Oshitani, Magnetic effects on thickness of adsorbed layer in aqueous solutions evaluated directly by atomic force microscope, J. Colloid Interface Sci. 204 (1998), https://doi.org/10.1006/jcis.1998.5590.
[60] S.R. Pruitt, K.R. Brorsen, M.S. Gordon, Ab initio investigation of the aqueous solvation of the nitrate ion, Phys. Chem. Chem. Phys. 17 (2015), https://doi.org/10.1039/c5cp04445f.
[61] O.F.González Vázquez, M.R.Moreno Virgen, M.S.Esparza González, V. Hernández Montoya, R. Tovar-Gómez, C.J.Durán Valle, Analysis of the effect of a magnetic field applied to a process of adsorption of water contaminants using adsorbents of different magnetic orderings 59 (2020), https://doi.org/10.1021/acs.iecr.0c00116.
[62] D.R. Lide, Magnetic susceptibility of the elements and inorganic compounds, CRC Handbook of Chemistry and Physics (2005).
[63] M.S. Afjeh, G.B. Marandi, M.J. Zohuriaan-Mehr, Nitrate removal from aqueous solutions by adsorption onto hydrogel-rice husk biochar composite, Water Environ. Res. 92 (2020) 934–947, https://doi.org/10.1002/wer.1288.
[64] M. Mossad, L. Zou, Evaluation of the salt removal efficiency of capacitive deionisation: kinetics, isotherms and thermodynamics, Chem. Eng. J. 223 (2013) 704–713, https://doi.org/10.1016/j.cej.2013.03.058.
[65] S.D. Kolev, Seven Years of Membranes: Feature Paper 2017, MDPI, 2018.
[66] L. Zhou, T. Li, J. An, C. Liao, N. Li, X. Wang, Efficient regeneration of activated carbon electrode by half-wave rectified alternating fields in capacitive deionization system, Electrochim. Acta 298 (2019) 372–378, https://doi.org/10.1016/j.electacta.2018.12.098.
[67] B. Sajjadi, W.-Y. Chen, N.O. Egiebor, A comprehensive review on physical activation of biochar for energy and environmental applications, Rev. Chem. Eng. 35 (2019) 735–776, https://doi.org/10.1515/revce-2017-0113.
[68] X. Yang, S. Zhang, M. Ju, L. Liu, Preparation and modification of biochar materials and their application in soil remediation, Appl. Sci. 9 (2019) 1365, https://doi.org/10.3390/app9071365.